Tube geometry can force switchlike transitions in the behavior of propagating bubbles

de Lozar, A. and Heap, A. and Box, F. and Hazel, A.L. and Juel, A.

2009

Manchester Institute for Mathematical Sciences

School of Mathematics

The University of Manchester

Tube geometry can force switchlike transitions in the behavior of propagating bubbles

A. de Lózar,[1,2] A. Heap,[1] F. Box,[1] A. L. Hazel,[1] and A. Juel[1]

[1]*Manchester Centre for Nonlinear Dynamics and School of Mathematics, University of Manchester, Oxford Road, Manchester M13 9PL, United Kingdom*
[2]*Max Planck Institute for Dynamics and Self-Organization, Bunsenstr. 10, Göttingen 37073, Germany*

Microscale process engineering requires precise control of bubbles and droplets. We investigate geometry-induced control and find that a centered constriction in the cross section of rectangular tubes can lead to new families of steadily propagating bubbles, which localize in the least-constricted regions of the cross section. Tuning the constriction geometry can cause a switchlike transition from centered to localized bubbles at a critical value of the flow rate: a mechanism for flow-rate-driven bubble control. The accompanying large change in bubble volume could be significant for liquid recovery applications. © *2009 American Institute of Physics.* [doi:10.1063/1.3247879]

The control of bubble and droplet traffic in microfluidic devices is an essential element of microscale process engineering and emerging lab-on-a-chip technologies,[1] but the development of efficient and effective control mechanisms requires a detailed understanding of the fundamental physics and chemistry occurring in two-phase flows at the microscale.[2] The generic two-phase flow underpinning droplet transport is the displacement of one fluid by another. This flow has a wide range of other applications, including oil extraction from porous reservoirs,[3] and the biomechanics of the lungs.[4] If air, for instance, is driven with a constant flow rate through a uniform tube initially filled with a viscous liquid, after a short distance, it forms a single finger that advances at constant speed, provided its speed is below the threshold for secondary instabilities. Surprisingly, this important interfacial flow has been studied only in tubes of simple geometries, i.e., circular, rectangular, or polygonal cross sections.[5–7] In most practical applications, however, the geometry of the tubes is considerably more complex, with areas of local constriction due to connecting or irregularly shaped pores in carbonate oil reservoirs,[8] and airway collapse or mucus build-up in the lungs.[9] Similarly in microchannels, the three-dimensional nature of the microfluidic network is often overlooked because bubble/droplet dynamics are generally visualized in a plane.[10–12] Rectangular channels are the norm, and the potential offered by more complex flow geometries has for the most part been neglected.

In this letter, we show that the centered constriction of the rectangular cross section of an axially uniform tube can lead to fundamental changes in the nature of bubble propagation within the tube, via the realization of new families of steadily propagating, asymmetric bubbles that localize in the least-constricted regions of the cross section. Moreover, the change from symmetric to asymmetric bubbles can be extremely abrupt: both types of bubbles are observed at a critical value of the flow rate, but their volumes per unit length differ by more than a factor of three. We demonstrate that this switchlike transition, which is robust over a wide range of tube geometries, is associated with a subcritical bifurcation that underpins the dynamics of bubble propagation in our system. Furthermore, we propose to exploit this switchlike transition as a powerful new means of manipulating and directing the transport of bubbles in microfluidic systems by variations in flow rate alone, without the need for any small-scale moving parts, electric/magnetic fields, lasers, or electronic valves.

We performed a series of experiments in rectangular tubes with an axially uniform, centered rectangular occlusion on the bottom surface of the tube, see Fig. 1(a) (inset). The height of the tube was fixed at $b=3.077 \pm 0.009$ mm, sufficiently large to allow the introduction of a range of occlusion heights, and the tube width was varied between $w=9-18$ mm, giving aspect ratios of $3<\alpha=w/b<6$, typical of microfluidic channels. The tubes consisted of two horizontal, 60 cm long float-glass sheets separated by precision-machined stainless steel strips and were uniform to less than 0.3% and 0.8% of their heights and widths, respectively.[13] Two different occlusions were used, $4.38 \pm 0.05 \times 1.005 \pm 0.016$ mm^2 and $4.50 \pm 0.01 \times 1.398 \pm 0.027$ mm^2 (width$\times$height). The occlusions were machined from Perspex to enable direct visualization, and they were bonded to the bottom glass plate of the tube to yield a 50 cm long axially uniform tube with a locally constricted cross section. The errors in the positional accuracy and axial uniformity of the occlusions were less than 0.5% and 3% of the occlusion width, respectively.

Initially, each tube was completely filled with silicone oil (viscosity of 50 cS). A two-phase displacement flow was induced by using a syringe pump to withdraw liquid from one end of the tube at a constant volumetric flow rate while leaving the other end open to the atmosphere. The induced flow consisted of a long bubble of air that propagated steadily, following the decay of initial transients. Over a small range of applied flow rates near bifurcations to localized bubbles, these transients could extend beyond the length of the tube, but for all other flow rates (away from bifurca-
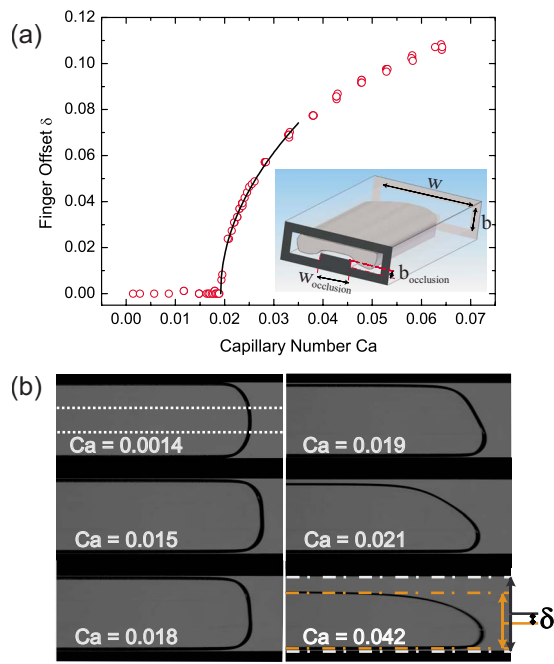
FIG. 1. (Color online) (a) Dimensionless air finger offset (see text) as a function of the capillary number. The line is a fit proportional to $\sqrt{Ca-Ca_c}$, which assumes a pitchfork bifurcation and yields $Ca_c=(1.92\pm0.04)\times10^{-2}$. Note that unavoidable imperfections bias the localized finger tip systematically toward the same side of the tube. (b) Top-view images of steadily propagating air fingers (left to right) in a tube with a locally constricted cross section [see inset in (a) for the tube geometry] of aspect ratio $\alpha=4.5$, dimensionless obstacle width $W=0.33$, and dimensionless obstacle height $B=0.33$. The occlusion is outlined with dotted lines in the first image.

tion points), they decayed over very short distances. The motion of the steady bubbles was recorded near the downstream end of the tube with a top-view camera (10 frames/s) over a distance of 4 cm ending 42.5 cm from the inlet. The bubble velocity was measured from the differences in position of the tip between frames.

Figure 1 shows the behavior of the system for increasing flow rates in a tube with the smaller occluded volume, in which the occlusion occupies approximately one third of the total width and height of the cross section (dimensionless occlusion width $W=w_{occlusion}/w=0.33$, dimensionless occlusion height $B=b_{occlusion}/b=0.33$). The non-dimensional bubble speed, $Ca=\mu U/\sigma$, known as the capillary number, can be interpreted as the ratio of viscous to surface tension forces, where U is the bubble speed, $\mu=5.4\times10^{-2}$ kg m^{-1} s^{-1} and $\sigma=2.1\times10^{-2}$ N m^{-1} are the dynamic viscosity and surface tension of the silicone oil, respectively. At low capillary numbers the entire bubble is symmetric about the vertical center plane of the tube and occupies the entire width of the tube (to within experimental resolution).[14] As the capillary number increases, the bubble tip loses its symmetry about the vertical center plane and, eventually, the entire bubble localizes near one wall. The localization is quantified by a parameter $-0.5<\delta<0.5$, defined to be the offset from the middle of the bubble to the middle of the tube, divided by the tube width (measured at a distance of 3.55 cm behind the bubble tip where it had reached a constant width).[15]

Above a critical value of the capillary number, $Ca_c=(1.92\pm0.04)\times10^{-2}$, the relative offset, δ, is proportional to $\sqrt{Ca-Ca_c}$, consistent with the behavior of a supercritical pitchfork bifurcation. Measurements were not taken for $Ca-Ca_c<0.16\,Ca_c$ because the lengthening of transients linked to critical slowing down meant that steadily propagating states were not reached within the length of the constricted tube. The behavior for $Ca>Ca_c$ is associated with a fundamental change in the bubble configuration far behind the tip, which is distinct from the previously observed thin-wire perturbation of the bubble-tip in a cylindrical tube, which broke the symmetry of the tip but did not result in bubble localization.[16]

As Ca increases, the bubble narrows monotonically[6] and selects a path of least resistance by moving into one of the less constricted regions of the tube cross section, resulting in the observed bubble localization. A complete understanding of the detailed dynamics will require three-dimensional numerical simulations, but insight into the influence of the cross-sectional geometry can be gained by considering the shape of the steadily propagating bubble far behind its tip. In the absence of surface-tension-driven instabilities of the films, it is known that the system becomes axially uniform with no interface curvature in the axial direction.[6] Hence, the transverse cross section of the bubble must always approach a two-dimensional equilibrium configuration satisfying the Young–Laplace equation, i.e., the product of surface tension and curvature is balanced by the pressure difference across the interface. The curvature is set by an integral force balance over the entire bubble surface, including viscous normal stresses at the tip in the dynamic case $(Ca>0)$. In cross sections with a centered constriction, three new families of asymmetric static $(Ca=0)$ solutions to the Young–Laplace equation can be found if $B\geq1/3$, which correspond to (i) complete localization within one of the unconstricted regions of the cross section, (ii) partial localization, in which the bubble extends into the constricted region, and (iii) slight localization, in which the bubble spans the entire constricted region and one of the unconstricted regions, protruding only slightly into the other unconstricted region. All three possibilities are consistent with experimental observations. We speculate that the geometric range of existence of these asymmetric solutions underlies the observed symmetry-breaking bifurcations. Hence, a simple change in cross-sectional shape is sufficient to alter fundamentally the dynamics of bubble propagation, because the bubble can remain localized even far behind the tip. Moreover, the existence of asymmetric bubbles at $Ca=0$ suggests that locally constricted tube geometries could be of practical importance in microfluidics and liquid recovery applications, which are often characterized by very small values of Ca.

The character of the transition can be changed by altering the size of the occlusion. We consider variations in relative height and width of the occlusion. In Fig. 2, we compare results for $B=0.33$ and $B=0.45$ for the same width $W=0.33$. Although the bubble shape at low capillary numbers is different for higher occlusions (in this case the bubble is double tipped), a transition to localized bubbles is still observed. However, it is so abrupt that both centered and localized
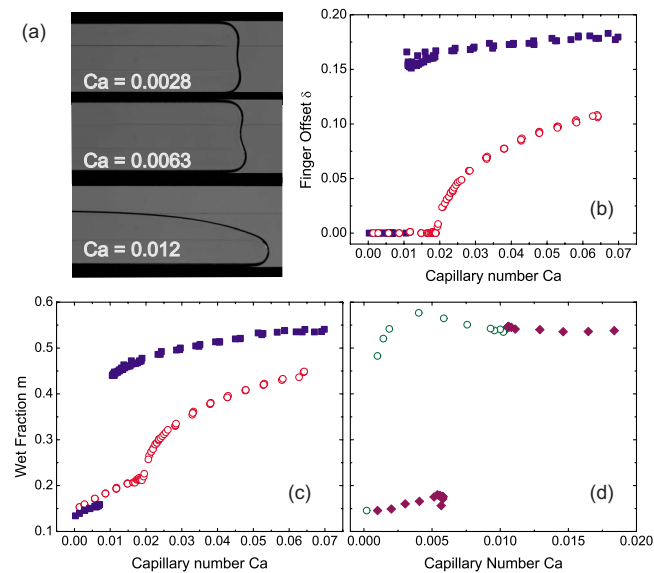
FIG. 2. (Color online) (a) Steady propagation of air fingers (right to left) for $\alpha=4.5$, $W=0.33$, and $B=0.45$. (b) Dimensionless air-finger offset as a function of Ca for $B=0.33$ [circles and previously shown in Fig. 1(b)] and $B=0.45$ (squares) with $W=0.33$ and $\alpha=4.5$. (c) Wet fraction as a function of Ca for the same parameters as in (b). (d) Wet fraction as a function of Ca for $B=0.45$, $W=0.25$, and $\alpha=6$. Diamonds depict experiments initiated from rest, while circles were obtained by reduction of the capillary number, starting with steady localized bubbles at $Ca=1.11\times10^{-2}$. The presence of hysteresis suggests a subcritical pitchfork bifurcation to localized bubbles.
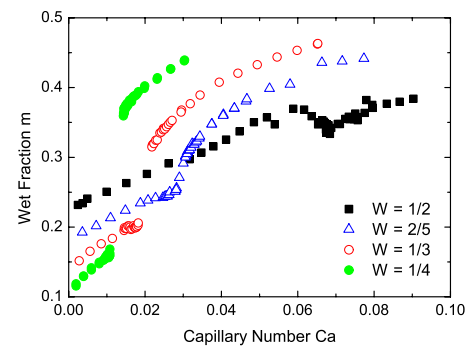

FIG. 3. (Color online) Wet fraction as a function of Ca for $B=0.33$ and $W=0.50$ (square), 0.40 (triangle), 0.33 (empty circle), and 0.25 (full circle). Fewer data points were taken in the transition region in this set of experiments, resulting in an apparent discontinuity at $W=0.33$, although the bifurcation is still supercritical. The bifurcation at $W=0.25$ is subcritical.

bubbles are observed at the same critical value of flow rate. Moreover, evidence of hysteresis was uncovered by establishing a steady, localized bubble and then reducing the flow rate to a value for which centered bubbles were usually observed, see Fig. 2(d). The presence of hysteresis suggests a transition from a supercritical to a subcritical pitchfork bifurcation with the increase in the occlusion height, which is often associated with tricritical phenomena.[17,18] In order to confirm that the observed behavior is not an artifact of the local measure δ, we also present results in terms of a global measure of the system, the so-called wet fraction, $m=1-\Phi/(AU)$, the ratio of the liquid volume that remains once the finger has exited the tube to the total volume of the tube. Above, Φ is the flow rate of the liquid and A is the cross-sectional area of the tube. The wet fraction exhibits a square-root variation with the excess parameter for $B=0.33$, but becomes discontinuous for $B=0.45$. The discontinuity in m may have implications for oil recovery applications, particularly in the highly irregular pore networks of carbonate rocks.[8] This is because, in our geometry, a small change in flow rate causes a 300% increase in the relative volume of oil remaining in the tube. Although pore-scale studies of multiphase flows in simple geometries are an established approach to gain insight into oil recovery,[19,20] the upscaling of our findings to an irregular porous structure is not trivial.

A similar transition from a supercritical to a subcritical bifurcation also takes place when the width of the tube is increased relative to the obstacle width. The variation of wet fraction with Ca shown in Fig. 3 indicates that the critical capillary number is shifted to lower values for the wider tube, suggesting that fine tuning of the geometry can be used

for precise control of the flow rate at which the transition occurs. The square-root behavior was observed to $W=0.40$, but for the narrowest tube ($W=0.50$), the bubble evolved continuously with increasing Ca. In contrast with the case when the obstacle height is varied, the bifurcation becomes subcritical for the narrower obstacle, where the tube is less occluded ($W=0.25$). Thus, even a small occlusion has a dramatic effect on the nature of the bubble propagation, for a wide enough tube.

In our system, gravitational and surface-tension forces are of approximately equal importance, as quantified by the Bond number, $Bo=\rho g b^2/\sigma=1.00\pm0.02$, where g is the acceleration due to gravity and ρ is the difference of density between the fluids. In microchannels, where typically $b\sim100$ μm, the Bond number is of the order of 10^{-3} and gravitational effects are negligible. A set of experiments in the same tube geometry as presented in Fig. 1, with the effect of gravity reduced by a factor of approximately 50 by using water rather than air ($Bo=0.02$), also showed transitions to localized bubbles. As in air, viscous stresses in the finger are not of major importance because the viscosity of the water is 50 times lower than the viscosity of the silicone oil. These results demonstrate that the phenomenon is robust and does not require the presence of gravitational forces. The localization is not independent of gravity, however, and the critical capillary number decreases to $Ca_c=(\mu_{sil}-\mu_{wat})U/\sigma_{wat-sil}=0.009\pm0.005$. The value of Ca_c is rather approximate because small water droplets, shed from the bubble, adhered to the channel walls, perturbing subsequent experiments.

The reduction in Ca_c with decreasing Bond number is a consequence of increased bubble surface area exposed to the obstacle as buoyancy effects become less important. This reduction in Ca_c and, more importantly, the existence of localized solutions to the Young–Laplace equations at $Ca=0$ suggest that a transition may be achievable in microfluidic channels where operating capillary numbers are typically 10^{-5}. The determination of a microfluidic geometry that can induce transitions as sharp and robust as those of the millimeter-scale experiments presented here remains an open challenge, particularly given that control of imperfections at microfluidic scales becomes more difficult.
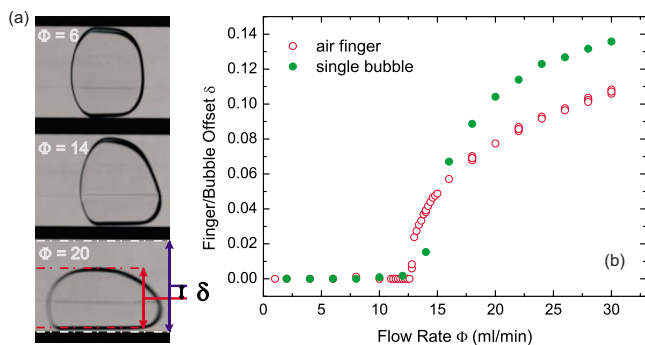
FIG. 4. (Color online) (a) Finite bubble in partially occluded tube with α =4.5, W=0.33, and B=0.33. (b) Offset for finite bubbles and fingers as a function of flow rate for α=4.5, W=0.33, and B=0.33. The bifurcation takes place at the same critical flow rate for fingers and finite bubbles, but the finite bubbles propagate at a lower speed due to the presence of a rear meniscus which causes additional viscous drag.

The results presented so far are for semi-infinite air fingers, but we also found that finite-length bubbles can exhibit localized states, shown in Fig. 4. Individual bubbles of length approximately equal to the width of the tube can be localized on one side of the tube. The critical flow rate remains approximately the same as that for the corresponding air finger, suggesting that the transition is governed by the hydrodynamic resistance of the tube's cross section. The propagation speed of a finite bubble is less than that of the long finger for the same flow rate due to the presence of a rear meniscus, inducing additional drag, and so the critical capillary number decreases. Decreasing the volume of the bubbles further will eventually lead to bubbles that are too small to be deformed by the tube geometry leading to a qualitative change in the dynamics because the bubbles will simply act as passive tracers and follow streamlines of the flow.

We propose that the switchlike localization of bubbles can be used to achieve traffic control at tube junctions by variation of flow rate alone. In a different set of experiments, the tube shown in Fig. 1 is connected to a Y-junction leading into two identical near-square daughter tubes. Long bubbles can be preferentially directed into either daughter tube by adjusting the flow rate. The transition occurs at the same value of flow rate as the symmetry-breaking bifurcation discussed above. Two movies illustrating the transition are provided in the supplementary materials.[21] This passive control mechanism is robust provided that the minimal but unavoidable asymmetries introduced in the manufacture of the obstacle and junction are deliberately biased to act in opposite directions. As bubbles tend to break at Y-junctions, a decelerating bubble in the second daughter tube accompanies the dominant accelerating bubble in our experiments. The same mechanism could, however, be used to direct trains of droplets and bubbles at T-junctions where short bubbles do not break.[22]

In conclusion, we have shown that a simple geometric modification can lead to fundamental changes in the dynamics of two-phase displacement flows within three-dimensional tubes. The robustness and simplicity of the observed switchlike transitions offer powerful new means of manipulating and directing bubbles in microchannels. Moreover, our findings suggest that in practical applications where tube geometries with many length scales dominate the two-phase flow dynamics, there could be at least threefold discrepancies in fluid recovery efficiencies compared to models that use tubes of simple geometries.

[1] G. M. Whitesides, "The origins and future of microfluidics," Nature (London) **442**, 368 (2006).

[2] M. Joanicot and A. Ajdari, "Droplet control for microfluidics," Science **309**, 887 (2005).

[3] G. M. Homsy, "Viscous fingering in porous media," Annu. Rev. Fluid Mech. **19**, 271 (1987).

[4] J. B. Grotberg and O. E. Jensen, "Biofluid mechanics of flexible tubes," Annu. Rev. Fluid Mech. **36**, 121 (2004).

[5] C. Clanet, P. Hérault, and G. Searby, "On the motion of bubbles in vertical tubes of arbitrary cross-sections: Some complements to the Dumitrescu–Taylor problem," J. Fluid Mech. **519**, 359 (2004).

[6] A. de Lózar, A. Juel, and A. L. Hazel, "The steady propagation of an air finger into a rectangular tube," J. Fluid Mech. **614**, 173 (2008).

[7] G. I. Taylor, "Deposition of viscous fluid on the wall of a tube," J. Fluid Mech. **10**, 161 (1961).

[8] N. Wardlaw, "The effects of pore structure on displacement efficiency in reservoir rocks and in glass micromodels," SPE Publication, Paper No. 8843 (1980).

[9] A. Heap and A. Juel, "Anomalous bubble propagation in elastic tubes," Phys. Fluids **20**, 081702 (2008).

[10] S. L. Anna, N. Bontoux, and H. A. Stone, "Formation of dispersions using "flow focusing" in microchannels," Appl. Phys. Lett. **82**, 364 (2003).

[11] F. Jousse, R. Farr, D. R. Link, M. J. Fuerstman, and P. Garstecki, "Bifurcation of droplet flows within capillaries," Phys. Rev. E **74**, 036311 (2006).

[12] C. Ody, C. N. Baroud, and E. de Langre, "Transport of wetting liquid plugs in bifurcating microfluidic channels," J. Colloid Interface Sc. **308**, 231 (2007).

[13] A. de Lózar, A. L. Hazel, and A. Juel, "Scaling properties of coating flows in rectangular channels," Phys. Rev. Lett. **99**, 234501 (2007).

[14] Silicone oil wets the tube walls, so films of oil are left behind on the side walls of the tube, but are so thin that they cannot be resolved experimentally.

[15] The value of δ may be either positive or negative depending on which side of the tube the finger localizes. We checked that the sign was determined by the unavoidable bias in the positioning of the occlusion by imposing a deliberate bias that switched the sign of δ.

[16] R. M. Fearn, "Perturbed motions of a bubble rising in a vertical tube," Phys. Fluids **31**, 238 (1988).

[17] A. Aitta, G. Ahlers, and D. S. Cannell, "Tricritical phenomena in rotating Couette–Taylor flow," Phys. Rev. Lett. **54**, 673 (1985).

[18] T. B. Benjamin and T. Mullin, "Anomalous modes in the Taylor experiment," Proc. R. Soc. Lond. A Math. Phys. Sci. **377**, 221 (1981).

[19] V. S. Ajaev and G. M. Homsy, "Modeling shapes and dynamics of confined bubbles," Annu. Rev. Fluid Mech. **38**, 277 (2006).

[20] W. L. Olbricht, "Pore-scale prototypes of multiphase flow in porous media," Annu. Rev. Fluid Mech. **28**, 187 (1996).

[21] See EPAPS supplementary material at http://dx.doi.org/10.1063/1.3247879 for movies of the experiments.

[22] D. R. Link, S. L. Anna, D. A. Weitz, and H. A. Stone, "Geometrically mediated breakup of drops in microfluidic devices," Phys. Rev. Lett. **92**, 054503 (2004).